

Fermion Masses in $SO(10)$ Models

Anjan S. Joshipura^a and Ketan M. Patel^b

Physical Research Laboratory, Navarangpura, Ahmedabad-380 009, India.

Abstract

We examine many $SO(10)$ models for their viability or otherwise in explaining all the fermion masses and mixing angles. This study is carried out for both supersymmetric and non-supersymmetric models and with minimal $(10 + \overline{126})$ and non-minimal $(10 + \overline{126} + 120)$ Higgs content. Extensive numerical fits to fermion masses and mixing are carried out in each case assuming dominance of type-II or type-I seesaw mechanism. Required scale of the $B - L$ breaking is identified in each case. In supersymmetric case, several sets of data at the GUT scale with or without inclusion of finite supersymmetric corrections are used. All models studied provide quite good fits if the type-I seesaw mechanism dominates while many fail if the type-II seesaw dominates. This can be traced to the absence of the $b-\tau$ unification at the GUT scale in these models. The minimal non-supersymmetric model with type-I seesaw dominance gives excellent fits. In the presence of a 45_H and an intermediate scale, the model can also account for the gauge coupling unification making it potentially interesting model for the complete unification. Structure of the Yukawa coupling matrices obtained numerically in this specific case is shown to follow from a very simple $U(1)$ symmetry and a Froggatt-Nielsen singlet.

PACS numbers: 12.10.-g, 12.15.Ff, 12.60.Jv, 14.60.Pq

^a anjan@prl.res.in

^b kmpatel@prl.res.in

I. INTRODUCTION

Grand unified theories (GUTs) which unify strong and electroweak interactions also provide a constrained and unified description of the fermion masses and mixing angles. This is particularly true in case of theories based on the $SO(10)$ group [1]. All the known fermions plus the right handed (RH) neutrino of a given generation are unified into a single spinorial 16-dimensional representation of the group. As a consequence, in a renormalizable theories of this type only three Yukawa coupling matrices Y_{10} , $Y_{\overline{126}}$, Y_{120} and relative strengths between them determine six physical mass matrices M_f with $f = u, d, l$ denoting quarks and the charged leptons, $f = D$ corresponding to the Dirac mass matrix for neutrinos and $f = L, R$ denoting the corresponding Majorana mass matrices for the left handed and right handed neutrinos respectively. The labels 10, $\overline{126}$, 120 correspond to three possible Higgs representations contained in the product $\overline{16} \times \overline{16}$. The presence of all these Higgs fields is not necessary and more economical and allowed possibility is to choose only two of them namely, 10 and $\overline{126}$. The consistent $SO(10)$ breaking needs additional Higgs representations - 210 or $210 + 54$ - in case of supersymmetric theories [2] and 45 in case of the non-supersymmetric $SO(10)$ model.

The minimal supersymmetric $SO(10)$ model with Higgs fields transforming as 10, $126 + \overline{126}$, 210 has limited numbers of free parameters and is explored in all its details [3–7]. Detailed analysis of fermion spectrum is also presented in case of the non-supersymmetric model containing an additional Higgs field in the 120 representation of $SO(10)$ [8–15]. Similar analysis in case of non-supersymmetric $SO(10)$ model is not done and the main purpose of the present paper is to provide such an analysis although we also give a comprehensive discussion of various numerical fits in the supersymmetric models.

The non-supersymmetric GUTs do not have built-in explanation of the gauge hierarchy problem but they do share several nice features of the supersymmetric models and avoid some of the problems associated with the latter. They allow gauge coupling unification [16] and can also provide dark matter candidate in the form of axion. In fact, a minimal non-supersymmetric $SO(10)$ model has been revived in recent studies [16, 17]. Earlier discussion of gauge coupling unification in such models is given in [18]. The minimal model is more economical than the corresponding supersymmetric case as far the choice of Higgs representation is concerned and uses only three sets of Higgs fields namely 10_H , $\overline{126}_H$ and 45_H . This choice is argued to lead to successful $SO(10)$ model on two counts:

(A) Two or three steps breaking of $SO(10)$ to the standard model (SM) is possible through the vacuum expectation value (vev) of 45_H and $\overline{126}_H$. An intermediate scale $\sim 10^{11}$ GeV allows the gauge coupling unification. This is shown through a detailed analysis using two loop renormalization group equations [16]. The presence of intermediate scales is also welcome from the point of view of explaining neutrino masses. This is unlike the minimal supersymmetric model where an intermediate scale required for neutrino masses spoils the

gauge coupling unification.

(B) The minimal model is argued [17] to be complete to the extent that the required pattern of the Higgs vacuum expectation values for the gauge symmetry breaking and gauge coupling unification can emerge from the minimization of the 1-loop corrected Higgs potential.

The fermion masses in the minimal supersymmetric or non-supersymmetric models arise from the following terms

$$16_F(Y_{10}10_H + Y_{\overline{126}}\overline{126}_H)16_F \quad (1)$$

The above terms represent a part of the superpotential in the supersymmetric case. In the non-supersymmetric version, one would need additional Peccei-Quinn like symmetry and the above terms would then represent the most general allowed fermion mass terms in the model. Two important features of eq.(1) are the following.

1. If the contribution of Y_{10} to the masses of the third generation dominates then one gets the b - τ unification

$$Y_b = Y_\tau \quad (2)$$

This can lead to large atmospheric mixing if neutrinos obtain their masses from the type-II seesaw mechanism [3].

2. Non-leading contribution to the second generation masses coming from $\overline{126}_H$ imply a relation

$$m_\mu = 3m_s \quad (3)$$

between the muon and the strange quark masses.

Both these relations are regarded as successful classical predictions of GUTs like $SO(10)$ [1] or $SU(5)$ a la Georgi-Jarlskog [20]. They are supposed to hold at the grand unification scale M_X . The available experimental information does not quite agree with these generic predictions at the quantitative level. Extrapolation of the quark masses at the GUT scale in the non-supersymmetric theories do not show b - τ unification. In supersymmetric theories, the evolved values of the Yukawa couplings depend on $\tan\beta$ and it is found that eq.(2) holds only at some special values of $\tan\beta$. Moreover, the presence of supersymmetry breaking around weak scale introduces additional finite $\tan\beta$ and sparticle mass-dependent corrections which need to be included in extrapolation. Eq.(3) also gets violated in a large parameter space at M_X in these theories. Several existing analysis of fermion masses in supersymmetric models [4–6, 9–11, 15] are based on simple and somewhat old extrapolation of fermion masses presented in [21] which does not include finite threshold corrections. As far as the non-supersymmetric theories are concerned there has not been any exhaustive confrontation of the extrapolated values [22] of fermion masses and mixing with the simple $SO(10)$ based models. Motivated by this, we address three main issues in this paper. (1) We update the existing analysis of fermion spectrum in various supersymmetric models using the recent extrapolation of fermion masses and mixing at the GUT scale [23, 24]. (2) We

provide new fitting of the fermion spectrum in various non-supersymmetric models and (3) try to understand the fitted structure of fermion mass matrices in terms of simple patterns. This provides hint into possible flavour structure of fermion spectrum and possible origin of large leptonic mixing angles.

We begin by giving an overview of the existing analysis of fermion masses and mixing. Then we discuss our fits in supersymmetric models. Here we consider both the minimal and the non-minimal models. Similar analysis is then carried out in Section IV in the non-supersymmetric case using the input from [22]. The analysis in these two sections demonstrates the viability or otherwise of various $SO(10)$ models from the point of obtaining correct fermion spectrum. In addition, it leads to very interesting structure for fermion mass matrices which can be a starting point to uncover the underlying flavour symmetries. We identify such structures in Section V and present a summary of all the new results of our analysis in Section VI.

II. OVERVIEW

Masses of fermions belonging to 16-dimensional spinorial representation of $SO(10)$ arise from the renormalizable couplings with Higgs fields belonging to $\overline{16} \times \overline{16} = 10 + \overline{126} + 120$ representations

$$16_F(Y_{10}10_H + Y_{\overline{126}}\overline{126}_H + Y_{120}120_H)16_F \quad (4)$$

in a self explanatory notation. The above couplings represent terms of the superpotential in case of supersymmetric models and Yukawa interactions in case of non-supersymmetric models with Peccei-Quinn symmetry, see latter. $(Y_{120}), Y_{10}, Y_{\overline{126}}$ are complex (anti)symmetric matrices in generation space. The Higgs fields $10_H + \overline{126}_H + 120_H$ are forced to be complex in case of the supersymmetric theories. The 10_H and 120_H representations of Higgs fields can be real in non-supersymmetric models but we shall take them to be complex in this case also to allow for the PQ symmetry. Throughout this paper, we shall restrict to the renormalizable models. There exists detailed analysis [25] of fermion masses in non-renormalizable models as well. The $10_H, \overline{126}_H, 120_H$ respectively contain 1, 1 and 2 up-like and equal number of down like Higgs doublets. It is assumed that only one linear combination of each remains light and acquires vacuum expectation value. This results in the following fermionic mass

matrices [9–11]:

$$\begin{aligned}
M_d &= H + F + iG , \\
M_u &= r(H + sF + it_u G) , \\
M_l &= H - 3F + it_l G , \\
M_D &= r(H - 3sF + it_D G) , \\
M_L &= r_L F , \\
M_R &= r_R^{-1} F .
\end{aligned} \tag{5}$$

where $(G) H, F$ are complex (anti)symmetric matrices. $r, s, t_l, t_u, t_D, r_L, r_R$ are dimensionless complex parameters of which r, r_L, r_R can be chosen real without loss of generality. The effective neutrino mass matrix for three light neutrinos resulting after the seesaw mechanism can be written as

$$\mathcal{M}_\nu = r_L F - r_R M_D F^{-1} M_D^T \equiv \mathcal{M}_\nu^{II} + \mathcal{M}_\nu^I . \tag{6}$$

Eqs.(5,6) describe the most general mass matrices in any renormalizable $SO(10)$ models and contain a large number of parameters to be of use. Therefore various special cases are considered in the literature and we summarize them below.

A. Minimal Supersymmetric Model

This model is characterized by the absence of 120_H and hence G in eq.(5). H can be diagonalized with real and positive eigenvalues by rotating the original 16-plets in the generation space. Hence all the mass matrices are determined by 19 real parameters if only type-II or type-I seesaw dominates. These parameters are determined using 18 observable quantities. In spite of the number of observables being less than the parameters, not all observables can be fitted with required precision due to non-linear nature of eq.(5). Eqs.(5) (with $G = 0$) are fitted to the observed fermion parameters in various papers [4–6]. The most general minimization is performed by Bertolini *et al* [4] allowing for arbitrary combination of both the type-I and II seesaw contributions to neutrino masses. The input values for quark and the charged lepton masses used in this analysis is taken from [21] and correspond to $\tan \beta = 10$. The best fits are obtained in a mixed scenario, type-I gives slightly worse and type-II scenario is unable to reproduce all the observables within 1σ . If type-II seesaw dominates then one needs b - τ unification at the GUT scale in order to reproduce large atmospheric mixing angle. In contrast, the extrapolated values used in the analysis do not show complete b - τ unification. This results in a poor fit to the atmospheric mixing angle at the minimum. Threshold effects can play important role in achieving the b - τ unification and improves the fit to fermion masses compared to analysis in [6] as we shall see.

B. Non-minimal supersymmetric model

The other case extensively discussed in the literature corresponds to adding a 120-plet of Higgs to the minimal model. Fermion masses in models in this category have been analyzed either assuming type-I [9–11, 14] or type-II [8, 9, 12, 13, 15] seesaw dominance. In this case, the most general model assuming type-II (type-I) dominance has 29 (31) independent parameters after rotating to basis with a real and diagonal diagonal H . One needs to make additional assumptions in order to reduce the parameter space. Considerable reduction in number of parameters is achieved assuming parity symmetry [13] or equivalently spontaneous CP violation [11]. This leads to Hermitian Dirac mass matrices. In our notation, this corresponds to taking all the parameters in eq.(5) to be real, see [9, 11] for details. Such a model has only 17 parameters in case of the type-II dominance, two less than in case of the minimal model without G but with arbitrary complex parameters. Number of parameters can be further reduced by imposing additional discrete symmetry; Z_2 [10] or μ - τ [9] are considered in this context. In spite of the reduction in number of parameters the allowed fermionic structure is analytically argued [12, 13] to help in reducing tension in obtaining correct CP violating phase or fitting the first generation masses.

Numerical fits depend on whether type-II or type-I seesaw mechanism is used. Comparison of various models in case of the type-II seesaw dominance is made in [15]. All the models in this category give a very good fit to data with a significantly lower χ^2 than in case of the minimal model. The assumption of the type-I dominance leads to better fits compared to the type-II case. Moreover, unlike the type-II dominance, one does not need intermediate scale [9–11, 14] for reproducing the correct neutrino mass scale. This is a welcome feature from the point of view of obtaining the gauge coupling unification. All these works are based on the use of quark masses derived in [21] at $\tan\beta = 10$. We shall re-examine the non-minimal model with a different set of input which include the finite threshold corrections.

C. Non-supersymmetric $SO(10)$ models

One common feature of all fits with type-II seesaw dominated scenarios is the need for an intermediate scale $M_I \sim 10^{12} - 10^{14}$ GeV. This spoils the gauge coupling unification in supersymmetric theories. In contrast, an intermediate scale in non-supersymmetric framework helps in achieving the gauge coupling unification. But unlike the supersymmetric case, the non-supersymmetric models do not show the b - τ unification and thus type-II models in this category do not immediately explain the large atmospheric neutrino mixing angles. Viability of this scenario can be checked through detailed numerical fits. Unlike the SUSY case, there is no systematic and complete three generation analysis of fermion masses within non-supersymmetric models. Various issues involved are summarized in a recent paper [26] which contains analytic discussion of the simplified two generation case.

The most economical possibility for fermion masses and mixing in non-supersymmetric model would be to choose a real 10_H or 120_H and $\overline{126}_H$ multiplets of Higgs fields. The latter is required for neutrino mass generation but by itself, it cannot generate fermion mixing. Thus additional 10_H or 120_H field is also needed. It is argued [26] that a $\overline{126}_H$ and a real 10_H cannot fit even two generation case. Thus one needs a complex 10_H . Since both the real and the imaginary parts of 10_H can independently couple to fermions, this would mean additional Yukawa couplings. This can be avoided by assigning a Peccei-Quinn (PQ) charge to 10_H . Consider the following general definition of the PQ symmetry:

$$\begin{aligned} 16_F &\rightarrow e^{i\alpha} 16_F; & \overline{126}_H &\rightarrow e^{-2i\alpha} \overline{126}_H \\ 10_H &\rightarrow e^{-2i\alpha} 10_H; & 120_H &\rightarrow e^{-2i\alpha} 120_H \end{aligned} \quad (7)$$

The most general Yukawa couplings allowed by this symmetry once again reduce to eq.(5). Thus formally both supersymmetric and non-supersymmetric cases look alike. But there is an important difference. The renormalization group running of the Yukawa couplings is different in these two cases. Moreover the non-supersymmetric case has intermediate scales. Thus input values and consequently the resulting fits would be quite different in these two cases.

III. FERMION MASSES IN SUPERSYMMETRIC THEORIES: NUMERICAL ANALYSIS

In this section, we present the numerical analysis of fermion masses and mixing in different supersymmetric cases. We use the data in Table(I) and define the following χ^2 function

$$\chi^2 = \sum_i \left(\frac{P_i - O_i}{\sigma_i} \right)^2, \quad (8)$$

where the sum $i = 1, \dots, 14$ runs over seven mass ratios and four quark mixing parameters (given in Table(I)), ratio of the solar to atmospheric mass squared differences and the solar (θ'_{12}) plus the atmospheric (θ'_{23}) mixing angles [27]. For the latter we use the values given in [28]. These data are fitted by numerically minimizing the function χ^2 . We assume Δm_{atm}^2 to be positive corresponding to the normal neutrino mass hierarchy. We also impose the 3σ upper bound on θ_{13} while minimizing the χ^2 . P_i denote the theoretical values of observables determined by the input expression, eq.(5) and O_i are the experimental values extrapolated to the GUT scale. σ_i denote the errors in O_i .

A. Minimal Supersymmetric model

Our input values of the quark masses and mixing angles at the GUT scale are based on the analysis in [23]. This uses more precise values of the b and t quark masses and the CKM parameters. More importantly, finite threshold corrections induced by sparticles are included in this analysis. Analysis in [23] proceeds in two steps. First, the quark masses and mixing angles are determined by fitting the available low energy data and evolving them to the supersymmetry breaking scale M_S . In the second step, finite sparticle induced corrections are included and then evolution is performed up to the GUT scale M_X . These corrections are expressed in terms of phenomenological parameters $\gamma_{d,b,u,t}$ defined below. We reproduce their table of values so obtained as Table(I) for convenience of the reader.

	A	B	C	D	C1	C2
$\tan \beta$	1.3	10	38	50	38	38
γ_b	0	0	0	0	-0.22	+0.22
γ_d	0	0	0	0	-0.21	+0.21
γ_t	0	0	0	0	0	-0.44
$y^t(M_X)$	6_{-5}^{+1}	0.48(2)	0.49(2)	0.51(3)	0.51(2)	0.51(2)
$y^b(M_X)$	$0.0113_{-0.01}^{+0.0002}$	0.051(2)	0.23(1)	0.37(2)	0.34(3)	0.34(3)
$y^\tau(M_X)$	0.0114(3)	0.070(3)	0.32(2)	0.51(4)	0.34(2)	0.34(2)
Observables	GUT scale values with propagated uncertainty					
(m_u/m_c)	0.0027(6)	0.0027(6)	0.0027(6)	0.0027(6)	0.0026(6)	0.0026(6)
(m_d/m_s)	0.051(7)	0.051(7)	0.051(7)	0.051(7)	0.051(7)	0.051(7)
(m_e/m_μ)	0.0048(2)	0.0048(2)	0.0048(2)	0.0048(2)	0.0048(2)	0.0048(2)
(m_c/m_t)	$0.0009_{-0.00006}^{+0.001}$	0.0025(2)	0.0024(2)	0.0023(2)	0.0023(2)	0.0023(2)
(m_s/m_b)	0.014(4)	0.019(2)	0.017(2)	0.016(2)	0.018(2)	0.010(2)
(m_μ/m_τ)	0.059(2)	0.059(2)	0.054(2)	0.050(2)	0.054(2)	0.054(2)
(m_b/m_τ)	$1.00_{-0.4}^{+0.04}$	0.73(3)	0.73(3)	0.73(4)	1.00(4)	1.00(4)
$\sin \theta_{12}^q$	0.227(1)	0.227(1)	0.227(1)	0.227(1)	0.227(1)	0.227(1)
$\sin \theta_{23}^q$	$0.0289_{-0.00073}^{+0.0179}$	0.0400(14)	0.0386(14)	0.0371(13)	0.0376(19)	0.0237(18)
$\sin \theta_{13}^q$	$0.0026_{-0.00045}^{+0.0022}$	0.0036(7)	0.0035(7)	0.0033(7)	0.0034(7)	0.0021(5)
$\delta_{CKM}[\circ]$	56.31 ± 10.24	56.31 ± 10.24	56.31 ± 10.22	56.31 ± 10.22	56.31 ± 10.27	56.31 ± 10.25

TABLE I. The input values of various observables of quark sector and charged lepton masses obtained at GUT-scale M_X for various values of $\tan \beta$ and threshold corrections $\gamma_{t,b,d}$ assuming an effective SUSY scale $M_S = 500$ GeV (see [23] for details).

Column (A)-(D) show the evolved values of quark mass ratios and mixing angles in the absence of threshold corrections for various values of $\tan \beta$. One clearly sees the absence of the b - τ unification at the GUT scale except for the low value of $\tan \beta$. This changes with the inclusion of threshold corrections. These corrections are parameterized by $\gamma_{d,u,b,t}$

which are defined in the following manner. The down quark mass matrix is determined by the term $QY_d d^c H_d$ in the minimal supersymmetric standard model. The corresponding term $QY'_d d^c H_u^*$ involving the second doublet H_u^* is not allowed in the superpotential by SUSY but it can be radiatively generated after the SUSY breaking. Since $\tan \beta \equiv \frac{\langle H_u^0 \rangle}{\langle H_d^0 \rangle}$, such terms give significant corrections to the tree level values for large $\tan \beta$ and should be included in evolving fermion masses and mixing from low energy scale to the M_X . The corrected down quark matrix is parameterized in [23, 29] by

$$U_L^{d\dagger} (1 + \Gamma^d + V_{CKM}^\dagger \Gamma_u V_{CKM}) Y_{\text{diag}}^d U_R^d$$

where $U_{L,R}^d$ and V_{CKM} are the (diagonal) down quark mass and the CKM matrix before the radiative corrections. The loops involving down squark-gaugino generate the second term and the loop with up squark-chargino generate the second term. $\Gamma_{d,u}$ are diagonal in the approximation of taking diagonal squark masses in the basis with diagonal quarks. Assuming equality of the first two generation squark masses, the diagonal elements $\Gamma_d = (\gamma_d, \gamma_d, \gamma_b)$ correct the down quark masses and $\Gamma_u = (\gamma_u, \gamma_u, \gamma_t)$ correct the CKM matrix in addition. The SUSY threshold corrections are included through these parameters and their best fit values corresponding to three classical GUT predictions namely eq.(2) and eq.(3) and the relation $\frac{m_d}{3m_e} = 1$ are determined. Last two columns correspond to different values of γ 's determined this way. Comparison of column C with C1,C2 shows that threshold corrections change significantly the b quark mass as well as $\theta_{23}^q, \theta_{13}^q$. The neutrino masses and mixing that we use are the updated low scale values [28] but the effects of the evolution to M_{GUT} on the ratio of the solar to atmospheric mass scale and on the mixing angles are known to be small for the normal hierarchical spectrum that we obtain here.

We now discuss detailed fits to fermion masses and mixing based on the input values in Table(I). We assume that either the type-I or the type-II seesaw term in the neutrino mass matrix dominates and carry out analysis separately in each of these two cases. We can rewrite eq(5) as follows.

$$\begin{aligned} M_u &= r m_\tau \left(\frac{3+s}{4} \tilde{M}_d + \frac{1-s}{4} \tilde{M}_l \right), \\ M_D &= r m_\tau \left(\frac{3(1-s)}{4} \tilde{M}_d + \frac{1+3s}{4} \tilde{M}_l \right), \\ M_L &= \frac{r_L m_\tau}{4} (\tilde{M}_d - \tilde{M}_l), \\ M_R &= \frac{r_R^{-1} m_\tau}{4} (\tilde{M}_d - \tilde{M}_l). \end{aligned} \tag{9}$$

We have chosen the basis with a diagonal M_l and introduced $\tilde{M}_{d,l} = \frac{1}{m_\tau} M_{d,l}$. Thus

$$\tilde{M}_l = \text{Diag.}(m_e/m_\tau, m_\mu/m_\tau, 1)$$

Hence all the quantities in the bracket in the above equation depend on the known ratios of charged lepton masses. \tilde{M}_d is a complex symmetric matrix with 12 real parameters. Since we

are fitting the ratios of different mass eigenvalues and mixing angles, the parameter r remains free and it can be fixed by m_t . r_L (r_R) in the case of type-II (type-I) seesaw dominance is determined from the atmospheric mass scale. We have total 14 real parameters (12 in \tilde{M}_d and complex s) which are fitted over 14 observables. Four unknown observables in lepton sector (θ_{13}^l and three CP violating phases) get determined at the minimum. Results of numerical analysis carried out separately for the type-II and the type-I dominated seesaw mechanisms are shown in Table(II) and Table(III) respectively. Let us comment on the results.

	A	B	C	D	C1	C2
Observables	Pulls obtained for best fit solution					
(m_u/m_c)	-0.00668428	0.0276825	0.0259467	0.120767	-0.0212532	0.0356043
(m_c/m_t)	0.56521	0.157569	0.0201093	0.0730136	0.130288	0.320944
(m_d/m_s)	-1.21642	-0.891034	-0.27664	-1.36265	-1.04724	-1.57673
(m_s/m_b)	0.112798	0.440678	0.163272	0.752408	0.884723	0.789053
(m_e/m_μ)	0.0590249	-0.00627804	0.3944	0.0396087	0.0297987	0.0555931
(m_μ/m_τ)	0.182548	0.103214	0.821485	0.0192305	0.26316	0.121145
(m_b/m_τ)	0.87282	2.20829	2.79368	2.34331	0.26656	0.407798
$\left(\frac{\Delta m_{sol}^2}{\Delta m_{atm}^2}\right)$	0.256292	0.116314	-0.14908	0.230056	0.0188227	-0.0140039
$\sin \theta_{12}^q$	0.0730813	0.0702755	0.0399788	0.105989	0.0779176	0.127757
$\sin \theta_{23}^q$	-0.0311676	-0.172792	-0.471738	-0.0960437	-0.757038	-0.945821
$\sin \theta_{13}^q$	1.33502	-0.0354198	0.494732	0.606606	0.890741	1.17758
$\sin^2 \theta_{12}^l$	0.00836789	-0.106439	-0.599727	-0.27881	-0.63356	-0.510182
$\sin^2 \theta_{23}^l$	-1.53367	-4.97038	-4.95673	-4.70944	-2.56294	-1.84412
$\delta_{CKM}[\circ]$	-0.345931	-0.163765	-0.600814	-0.214459	-0.650554	-0.75885
χ_{min}^2	6.9367	30.70	34.52	30.68	10.804	9.3559
Observables	Corresponding Predictions at GUT scale					
$\sin^2 \theta_{13}^l$	0.0226508	0.0190847	0.0206716	0.0196974	0.0239619	0.0209208
$\delta_{MNS}[\circ]$	19.9399	18.9784	19.5619	11.92	358.789	1.78569
$\alpha_1[\circ]$	337.171	346.627	344.795	350.595	12.4786	349.711
$\alpha_2[\circ]$	147.364	151.912	146.886	161.702	194.023	168.156
$r_L m_\tau [\text{GeV}]$	8.37×10^{-10}	6.0×10^{-10}	6.49×10^{-10}	6.94×10^{-10}	7.15×10^{-10}	9.1×10^{-10}

TABLE II. Best fit solutions for fermion masses and mixing obtained assuming the type-II seesaw dominance in the minimal SUSY $SO(10)$ model. Pulls of various observables and predictions obtained at the minimum are shown for six different data sets.

- The best fit in the type-II case is obtained at low $\tan \beta = 1.3$. This case has b - τ unification and threshold corrections are not very significant. On the other hand,

	A	B	C	D	C1	C2
Observables	Pulls obtained for best fit solution					
(m_u/m_c)	0.0486938	-0.180782	0.0653101	0.0053847	0.0467579	-0.0119661
(m_c/m_t)	1.22599	0.130589	0.246294	0.146932	0.297256	0.273346
(m_d/m_s)	-0.229546	-0.730641	0.223201	-0.748148	-2.2904	-0.689684
(m_s/m_b)	-0.932536	-0.886438	-0.977249	-1.05766	0.735548	0.000467775
(m_e/m_μ)	0.0340323	0.442759	0.103692	-0.476364	0.0649144	-0.0648856
(m_μ/m_τ)	0.310305	-0.526529	0.881934	0.938701	0.705648	0.0178824
(m_b/m_τ)	-0.486477	-0.194215	0.0172182	-0.34079	0.789868	-0.734937
$\left(\frac{\Delta m_{sol}^2}{\Delta m_{atm}^2}\right)$	0.122267	-0.10063	-0.00563647	-0.120429	-0.180164	0.158557
$\sin \theta_{12}^q$	0.0432634	0.227948	0.0186715	0.084149	0.130301	0.0922391
$\sin \theta_{23}^q$	-0.281221	-0.0401177	-0.167224	0.0649082	-0.273222	-1.17651
$\sin \theta_{13}^q$	1.37864	-0.275689	0.926186	0.559003	1.48675	0.248759
$\sin^2 \theta_{12}^l$	-0.0528379	-0.0598219	-0.38133	-0.172148	-0.746107	0.0694831
$\sin^2 \theta_{23}^l$	-1.22555	-1.27077	-1.43475	0.0548963	-1.99485	-0.946001
$\delta_{CKM}[\circ]$	-0.291137	0.397159	-0.350422	-0.755859	-0.956628	-0.3197
χ_{min}^2	6.3479	3.7962	5.0715	3.8665	14.789	3.4746
Observables	Corresponding Predictions at GUT scale					
$\sin^2 \theta_{13}^l$	0.0223307	0.0194886	0.0218753	0.0186789	0.0253152	0.0205366
$\delta_{MNS}[\circ]$	2.41793	4.52493	6.08769	335.07	357.142	14.7651
$\alpha_1[\circ]$	347.106	8.42838	7.64991	28.0261	14.5679	1.13126
$\alpha_2[\circ]$	163.759	191.241	188.713	218.586	196.273	177.828
$r_R \left(\frac{m_t^2}{m_\tau}\right)$ [GeV]	1.77×10^{-10}	2.63×10^{-10}	2.50×10^{-10}	4.02×10^{-10}	7.3×10^{-11}	2.82×10^{-10}

TABLE III. Best fit solutions for fermion masses and mixing obtained assuming the type-I seesaw dominance in the minimal SUSY $SO(10)$ model. Pulls of various observables and predictions obtained at the minimum are shown for six different data sets.

cases B, C, D with relatively large $\tan \beta$ but without inclusion of threshold correction give quite bad fit. There is a clear correlation between the overall fit and the presence or absence of the b - τ unification in type-II models. Cases corresponding to the absence of the b - τ unification cannot reproduce the atmospheric mixing angle and results in relatively poor fits. Inclusion of threshold corrections improves the fit but still $\frac{m_d}{m_s}$ and the atmospheric mixing angle cannot be reproduced within 1σ . The fit for $\tan \beta = 10$ obtained here with inputs from [23, 28] is poor compared to the corresponding fit presented in [6] which uses input from [21]. Compared to data in [21], the result from [23] display larger deviation from the b - τ unification and also errors in more recent input that we use for $\sin^2 \theta_{23}^l$ are smaller. Both these features combine to give larger

pulls for the ratio $\frac{m_b}{m_\tau}$ and $\sin^2 \theta_{23}^l$ and results in poor fit.

- In contrast to the type-II case, the fits obtained in type-I case are uniformly better. Here one does not expect correlation between the atmospheric mixing angle and b - τ unification. Thus the cases B, C, D with large $\tan \beta$ also give quite good fits. Even in these cases (except D) main contribution to χ^2 comes from the pull in the atmospheric mixing angle. Threshold corrections are significant for large $\tan \beta$ and specific cases C1, C2 achieve b - τ unification but the overall fit worsens compared to B, C, D. Unlike in the type-II case, the χ^2 value obtained here for $\tan \beta = 10$ is comparable to the corresponding value in [6].
- We have fixed the overall scale of neutrino mass $r_L(r_R)$ in the case of type-II (type-I) seesaw by using the atmospheric scale as normalization. The resulting values are displayed in Table(II, III). $r_L(r_R)$ arise from the vev of the components of $\overline{126}_H$ transforming as $(3, 1, -2)$ ($(1, 3, -2)$) under the $SU(2)_L \times SU(2)_R \times U(1)_{B-L}$. In particular, $\langle(1, 3, -2)\rangle_{\overline{126}_H}$ sets the scale of the $B - L$ breaking and is directly determined from the fits to fermion masses in the type-I scenario. From eq.(9),

$$\langle(1, 3, -2)\rangle_{\overline{126}_H} \approx r_R^{-1} v s_m \cos \beta , \quad (10)$$

where s_m gives the mixing of the light H_d in the doublet part of $\overline{126}_H$ and $v \approx 174$ GeV. r_R is roughly independent of the input data set and for the value $r_R \approx 2.6 \times 10^{-10} m_\tau / m_t^2$ GeV, eq.(10) gives

$$\langle(1, 3, -2)\rangle_{\overline{126}_H} \approx 3.7 \times 10^{15} s_m \cos \beta \text{ GeV}$$

Thus the $B - L$ breaking scale in the type-I seesaw can be close to the GUT scale for $s_m \cos \beta \sim \mathcal{O}(1)$. It would however be significantly lower for large values of $\tan \beta$ and would conflict with the constraints from the gauge coupling unification. The determination of the $B - L$ breaking scale in the type-II dominated scenario is dependent on the details of the superpotential. Earlier [5, 6] analysis in the minimal model has shown that this scale cannot easily be lifted to the GUT scale and poses a problem with the gauge coupling unification in the minimal scenario both for the type-I and type-II seesaw dominance [6]. Thus one does need to go beyond the minimal model and models with 120_H are possible examples.

B. Numerical Analysis: Extended model with $10 + \overline{126} + 120$ Higgs

We now consider the non-minimal case obtained from eq.(5) by choosing all parameters in H, F, G as well as $r, s, t_u, t_l, t_D, r_l, r_R$ real. As before, the parameters r and $r_R(r_L)$ determine the m_t and overall scale of neutrino masses in type-I (type-II) seesaw dominated scenarios. Our choice of 14 observables is the same as in the previous subsection. But they are now

determined from the more general expression with non-zero G . H can be made diagonal without loss of generality. The mass matrices M_u, M_d, M_l, M_D, M_R and M_L are expressed in terms of 16 real parameters (3 in H , 6 in F , 3 in G , s, t_l, t_u , and t_D) which determine 14 observables P_i defined before.

	A	B	C	D	C1	C2
Observables	Pulls obtained for best fit solution					
(m_u/m_c)	0.00196316	0.019005	-0.026015	-0.00109589	-0.00812155	0.0000225717
(m_c/m_t)	0.000750815	-0.114469	0.0964863	0.296526	-0.0278823	-0.00413523
(m_d/m_s)	0.0547314	0.618531	0.0606721	-1.14305	0.0271889	0.00312586
(m_s/m_b)	0.0565403	0.473347	-1.30774	0.675173	0.0105556	0.0361755
(m_e/m_μ)	0.0114456	-0.0155357	0.0482971	-0.00371258	0.00167012	0.000128709
(m_μ/m_τ)	-0.00279654	-0.66999	0.111235	-0.0605957	0.00155096	-0.00249006
(m_b/m_τ)	-0.171035	-0.301056	-0.381508	1.57926	0.0514536	-0.048487
$\left(\frac{\Delta m_{sol}^2}{\Delta m_{atm}^2}\right)$	0.00833338	-0.297416	0.191515	0.2129	0.00050834	-0.00412658
$\sin \theta_{12}^q$	-0.0106839	-0.0145213	-0.0420229	0.0809603	-0.00715584	0.0000538731
$\sin \theta_{23}^q$	-0.00295777	-0.058218	0.301593	0.341191	0.0120366	-0.000633901
$\sin \theta_{13}^q$	-0.00466345	-0.661544	0.381317	-0.632744	-0.137308	0.00650479
$\sin^2 \theta_{12}^l$	0.0106277	-0.194399	0.333404	0.399294	0.00217496	-0.0043514
$\sin^2 \theta_{23}^l$	-0.0198083	1.08433	-0.472589	-0.885401	0.0314484	0.00752103
$\delta_{CKM}[\circ]$	-0.00915099	0.168633	-0.520071	0.246618	-0.0314877	-0.0382519
χ_{min}^2	0.0364	2.9315	2.7639	5.921	0.0254	0.0038
Observables	Corresponding Predictions at GUT scale					
$\sin^2 \theta_{13}^l$	0.0215726	0.0312498	0.03568	0.0214329	0.0289663	0.0069694
$\delta_{MNS}[\circ]$	34.3864	5.21955	89.5	315.898	355.507	75.6953
$\alpha_1[\circ]$	6.26083	76.0772	289.921	80.1968	60.3609	240.526
$\alpha_2[\circ]$	161.011	253.288	76.0613	283.63	220.306	34.4702
$r_L m_\tau [\text{GeV}]$	1.27×10^{-9}	9.57×10^{-10}	6.82×10^{-10}	1.56×10^{-9}	2.36×10^{-9}	3.68×10^{-9}

TABLE IV. Best fit solutions for fermion masses and mixing obtained assuming the type-II seesaw dominance in the non-minimal SUSY $SO(10)$ model. Pulls of various observables and predictions obtained at the minimum are shown for six different data sets.

Results of numerical analysis carried out separately for the type-II and type-I dominated seesaw mechanisms are shown in Table(IV) and Table(V) respectively. The following remarks are in order in connection with the results presented in these tables. As discovered in earlier numerical analysis [9, 15], the introduction of the 120_H leads to remarkable improvement in numerical fits in the type-II case. This mainly arises because the near maximality θ_{23}^l is not directly connected to the b - τ unification. Thus the cases B, C, D which do not have the b - τ unification also lead to very good fits in contrast to the minimal case. The fits

	A	B	C	D	C1	C2
Observables	Pulls obtained for best fit solution					
(m_u/m_c)	-0.0151499	0.0262493	-0.0019449	-0.00461056	0.00542513	-0.0000775584
(m_c/m_t)	-0.000384519	0.000812518	0.000258262	0.00461629	-0.00304033	0.0049013
(m_d/m_s)	-0.0778857	-0.0653974	-0.0053692	0.0272334	0.00701785	0.00147573
(m_s/m_b)	-0.052311	0.0706689	0.0726379	0.0830354	0.0120634	0.0296307
(m_e/m_μ)	0.00127584	0.00152407	0.00164957	0.0268034	-0.00722174	-0.000349497
(m_μ/m_τ)	-0.0553488	-0.0188764	-0.0212797	-0.0282999	-0.00866254	-0.00875371
(m_b/m_τ)	-0.0103881	0.0214596	0.0260868	0.0498589	0.00493891	0.00967378
$\left(\frac{\Delta m_{sol}^2}{\Delta m_{atm}^2}\right)$	0.0324886	0.00926157	0.00312614	-0.00630473	-0.00302065	0.000653399
$\sin \theta_{12}^q$	0.0159112	-0.0140628	-0.000195379	0.00791696	-0.0171517	-0.000184021
$\sin \theta_{23}^q$	0.0375281	-0.00674466	-0.00216987	0.00501282	0.0100126	0.00590551
$\sin \theta_{13}^q$	0.0309917	0.0571306	0.175888	0.0213394	-0.131639	-0.00184989
$\sin^2 \theta_{12}^l$	0.00539037	-0.0176765	0.00577816	-0.013618	0.0092152	0.000404734
$\sin^2 \theta_{23}^l$	0.0332756	0.0143127	0.0125096	0.0200216	0.00356131	0.00026684
$\delta_{CKM}[\circ]$	-0.0585649	-0.00882152	-0.0406312	-0.0292954	-0.0291351	-0.0310722
χ_{min}^2	0.0204	0.0150	0.0392	0.0137	0.0191	0.0011
Observables	Corresponding Predictions at GUT scale					
$\sin^2 \theta_{13}^l$	0.0122064	0.0168745	0.0146633	0.0359278	0.0246489	0.030277
$\delta_{MNS}[\circ]$	87.6747	22.8731	330.351	282.035	272.186	84.0238
$\alpha_1[\circ]$	5.82048	167.229	192.077	286.062	352.828	329.804
$\alpha_2[\circ]$	339.846	331.88	34.5585	336.358	17.6585	325.182
$r_R \left(\frac{m_t^2}{m_\tau}\right) [\text{GeV}]$	6.56×10^{-15}	1.22×10^{-12}	1.34×10^{-12}	3.03×10^{-15}	5.0×10^{-14}	1.40×10^{-13}

TABLE V. Best fit solutions for fermion masses and mixing obtained assuming the type-I seesaw dominance in the non-minimal SUSY $SO(10)$ model. Pulls of various observables and predictions obtained at the minimum are shown for six different data sets.

in cases (A, C1, C2) which have b - τ unification are even better and all the observables are fitted almost exactly in these cases. These include the low $\tan \beta$ inputs and cases with large $\tan \beta$ and threshold corrections. As the results of Table(V) show, the fits obtained assuming the type-I seesaw dominance are uniformly better compared to the corresponding type-II results and show significantly improvement over the minimal model with type-I dominance, Table(III).

One important difference compared to the minimal case is the overall $B - L$ scale determined from the neutrino masses. Unlike the minimal case, the values of r_R^{-1} in Table(V) are strongly dependent on the input data set and in some cases are quite large although each

data set appear to give very good fit to fermion masses. For example, one obtains in case (A) from eq.(10) and Table(V),

$$\langle(1, 3, -2)\rangle_{\overline{126}_H} \approx 1.5 \times 10^{20} s_m \cos \beta \text{ GeV}$$

Thus reproducing neutrino masses in this case would require fine tuning $s_m \sim 10^{-4}$ if the $B - L$ breaking scale is to be close to M_{GUT} . In contrast, in case C2 with $\tan \beta = 38$, Table(V) gives

$$\langle(1, 3, -2)\rangle_{\overline{126}_H} \approx 1.8 \times 10^{17} s_m \text{ GeV}$$

which is close to the GUT scale.

IV. FERMION MASSES IN NON-SUPERSYMMETRIC MODELS: NUMERICAL ANALYSIS

We now turn to the discussion of various non-supersymmetric models. We shall consider three different cases.

1. The minimal scenario containing the Higgs representations $45_H + 10_H + \overline{126}_H$.
2. Alternative model with $45_H + 120_H + \overline{126}_H$ proposed and analyzed in case of two generations in [26]
3. The non-minimal scenario with $45_H + 10_H + \overline{126}_H + 120_H$ with Hermitian structure.

The case (2) is found to be unable to fit all the fermion masses and mixing angles. The minimal case works quite well in this regards and there is no real motivation to go to the non-minimal case as far as the fermion masses are concerned. We have included this for completeness and find that this case works even better than the minimal case.

The $SO(10)$ breaking [17] and the gauge coupling unification [16] with intermediate scale has been reanalyzed recently following earlier works [18, 19]. The minimal case is argued to be adequate in achieving both the gauge coupling unification and breaking of $SO(10)$ to the SM through an intermediate scale. The exact value of the required intermediate scale depend on the chain of the $SO(10)$ breaking and various cases are given in [16]. The 45_H field contains components transforming as (15,1,1) and (1,1,3) under the Pati-Salam group $SU(4) \times SU(2)_L \times SU(2)_R$. They allow $SO(10)$ braking to $SU(3)_C \times SU(2)_L \times SU(2)_R \times U(1)_{B-L}$, $SU(4) \times SU(2)_L \times U(1)_R$ or to $SU(5) \times U(1)$ groups. At the tree level, only $SU(5)$ intermediate stage is shown to lead to consistent spectra without tachyons [19] but this chain does not preserve the gauge coupling unification. As discussed in [17] turning on 1-loop corrections also allows the other two breaking chains which preserve gauge coupling unification. The final breaking to SM can be achieved by the (1,1,3) component

of $\overline{126}_H$ which also leads to neutrino masses. The 10_H and $\overline{126}_H$ contain respectively bi-doublets (1,2,2) and (15,2,2). They need to mix in order to finally generate the standard model doublet(s) simultaneously containing the 10_H and $\overline{126}_H$ components. This can be achieved by fine tuning. For example, the mixing between bi-doublets is achieved through the following term

$$V \sim \chi_{ij} \chi_{kl} \Sigma_{ijklm} \phi_m \quad (11)$$

which couples 45_H (χ) to $\overline{126}_H$ (Σ) and 10_H (ϕ). This mixes two bi-doublets when component of 45_H transforming as singlet under the $SU(3)_c \times SU(2)_L \times SU(2)_R \times U(1)_{B-L}$ acquires a vev. Then through fine tuning one can keep one of the two bi-doublets in 10_H and $\overline{126}_H$ at the intermediate scale. Subsequent breaking to SM is achieved through the (1, 1, 3) component of $\overline{126}_H$. Eq.(11) provides this way the required mixing between doublets in $\overline{126}_H$ and 10_H .

A. Numerical Analysis: Model with only $10 + \overline{126}$ Higgs fields.

A non-supersymmetric $SO(10)$ model with 10 and $\overline{126}$ Higgs fields together with $U(1)_{PQ}$ symmetry has the same Yukawa interactions as the minimal SUSY $SO(10)$, eq.(5) with $G = 0$. Minimization is performed based on the input values of the charged fermion masses obtained by running quark and lepton masses up to the GUT scale with $m_H=140$ GeV [22]. We use the updated low energy values of quark mixing angles, CP phase and neutrino parameters since the effect of RG is known to be negligible for hierarchical neutrino spectrum. We reproduce all the input values in Table(VI) for convenience. As before, we take M_d and M_l as independent and express the remaining matrices in terms of them and r, s as in eq.(9). Since the masses of the charged leptons are known precisely, we go to the basis with a diagonal M_l and use them as fixed input. Thus we have 15 real parameters (12 in M_d , complex s and real r) which determine remaining 13 observables shown in Table (VI). The χ^2 function is defined in terms of these parameters.

Results of numerical analysis carried out separately for type-I and type-II dominated seesaw mechanisms are shown in Table(VII). Parameters obtained for the best fit solutions are shown in Appendix A. It is evident that the type-II mechanism fails completely in reproducing the spectrum. Once again this is linked to the complete absence of the b - τ unification in non-supersymmetric theories. Neither the atmospheric mixing nor the b quark mass can be reproduced correctly in this fit. In contrast, the type-I seesaw works quite well. In fact, the quality of fit in this case is much better than the minimal supersymmetric model with type-I seesaw, Table (III).

As before the r_R gets determined from the atmospheric neutrino mass scale. Assuming, that only one standard model survives at the electroweak scale one has,

$$\langle (1, 3, -2) \rangle_{\overline{126}_H} \approx r_R^{-1} s_m v$$

GUT scale values with propagated uncertainty			
$m_d(\text{MeV})$	$1.14^{+0.51}_{-0.48}$	$\Delta m_{sol}^2 (\text{eV}^2)$	$(7.59 \pm 0.20) \times 10^{-5}$
$m_s(\text{MeV})$	22^{+7}_{-6}	$\Delta m_{atm}^2 (\text{eV}^2)$	$(2.51 \pm 0.12) \times 10^{-3}$
$m_b(\text{GeV})$	1.00 ± 0.04	$\sin \theta_{12}^q$	0.2246 ± 0.0011
$m_u(\text{MeV})$	$0.48^{+0.20}_{-0.17}$	$\sin \theta_{23}^q$	0.0420 ± 0.0013
$m_c(\text{GeV})$	$0.235^{+0.035}_{-0.034}$	$\sin \theta_{13}^q$	0.0035 ± 0.0003
$m_t(\text{GeV})$	$74.0^{+4.0}_{-3.7}$	$\sin^2 \theta_{12}^l$	0.3208 ± 0.0164
$m_e(\text{MeV})$	$0.469652046 \pm 0.000000041$	$\sin^2 \theta_{23}^l$	$0.4529^{+0.0924}_{-0.0484}$
$m_\mu(\text{MeV})$	99.1466226 ± 0.0000089	$\sin^2 \theta_{13}^l$	$< 0.049(3\sigma)$
$m_\tau(\text{GeV})$	1.68558 ± 0.00019	δ_{CKM}	$69.63^\circ \pm 3.3^\circ$

TABLE VI. Input values for quark and leptonic masses and mixing angles in the non-supersymmetric standard model extrapolated at $M_{GUT} = 2 \times 10^{16}$ GeV.

r_R in Table (VII) gives

$$\langle (1, 3, -2) \rangle_{\overline{126}_H} \approx 3 \times 10^{15} s_m \text{ GeV} . \quad (12)$$

Unlike the supersymmetric model, one would like to have this scale at an intermediate value 10^{11} GeV [16] in order to achieve the gauge coupling unification. This will require substantial fine tuning. The exact value of the required intermediate scale for the gauge coupling unification would depend on threshold effects not included in the analysis in [16]. This would need a detailed study of the scalar potential minimization and the scalar sector of the theory.

The leptonic parameters θ_{13} and three CP violating phases $\alpha_{1,2}$ and δ_{MNS} get fixed at the minimum and are shown in Table(VII). The firm predictions on these observables in the scheme can be obtained by checking the variation of χ^2 with the values of various observables. Following, [9, 11], we pin down a specific value p_0 of an observable P by adding a term

$$\chi_P^2 = \left(\frac{P - p_0}{0.01 p_0} \right)^2$$

to χ^2 and then minimizing

$$\hat{\chi}^2 \equiv \chi^2 + \chi_P^2 .$$

If P happens to be one of the observables used in defining χ^2 , then its contribution is removed from there. Artificially introduced small error fixes the value p_0 for P at the minimum of the $\hat{\chi}^2$. We then look at the variation of

$$\bar{\chi}_{min}^2 \equiv (\hat{\chi}^2 - \chi_P^2)|_{min} \quad (13)$$

with p_0 . The results of such analysis carried out for the observables $\sin^2 \theta_{23}^l$ and $\sin^2 \theta_{13}^l$ are displayed in Fig.1 and Fig.2 respectively. $\sin^2 \theta_{23}^l$ can assume value in large range and the 90% confidence level bound corresponding to $\Delta\chi^2 = 4.61$ covers its entire 3σ range

Observables	Type-I		Type-II	
	Fitted value	pull	Fitted value	pull
m_d	0.000810163	-0.687161	0.00101285	-0.264898
m_s	0.0208099	-0.198354	0.0225915	0.0844982
m_b	0.999667	-0.00831657	1.08201	2.05031
m_u	0.000495023	0.0751133	0.000507336	0.13668
m_c	0.237348	0.0670883	0.237096	0.0598882
m_t	73.9427	-0.0154941	74.3006	0.075144
m_e	0.000469652	-	0.000469652	-
m_μ	0.0991466	-	0.0991466	-
m_τ	1.68558	-	1.68558	-
$\left(\frac{\Delta m_{sol}^2}{\Delta m_{atm}^2}\right)$	0.030526	0.127968	0.0297114	-0.235285
$\sin \theta_{12}^q$	0.224651	0.0464044	0.224499	-0.0916848
$\sin \theta_{23}^q$	0.0420499	0.0392946	0.0421308	0.103004
$\sin \theta_{13}^q$	0.00349369	-0.0974312	0.00353053	0.0389979
$\sin^2 \theta_{12}^l$	0.323245	0.148134	0.3108	-0.610792
$\sin^2 \theta_{23}^l$	0.435096	-0.369178	0.113306	-7.02461
$\sin^2 \theta_{13}^l$	0.0244287	-	0.0176863	-
$\delta_{CKM}[\circ]$	69.5262	-0.0314447	69.2051	-0.128759
$\delta_{MNS}[\circ]$	318.465	-	14.5386	-
$\alpha_1[\circ]$	21.5053	-	345.645	-
$\alpha_2[\circ]$	215.128	-	141.905	-
$r_{R(L)}$	5.62×10^{-14}	-	2.09×10^{-10}	-
χ^2		0.710777		54.1197

TABLE VII. Best fit solutions for fermion masses and mixing obtained assuming the type-I and type-II seesaw dominance in the minimal non-SUSY $SO(10)$ model. Various observables and their pulls at the minimum are shown. All the masses shown are in GeV units. The bold faced quantities are predictions of the respective solutions.

0.33 – 0.64. In contrast, a clear prediction emerges for the angle $\sin^2 \theta_{13}^l$ which preferentially lies in the range 0.015 – 0.03.

B. Numerical Analysis: Model with only $120 + \overline{126}$ Higgs fields.

We now consider an alternative model obtained by replacing 10_H with 120_H in the minimal model discussed before. This model is argued to be quite attractive and predictive when restricted to the second and the third generations [26]. It is thus interesting to see if the model works in more realistic case with three generations which require explanation of

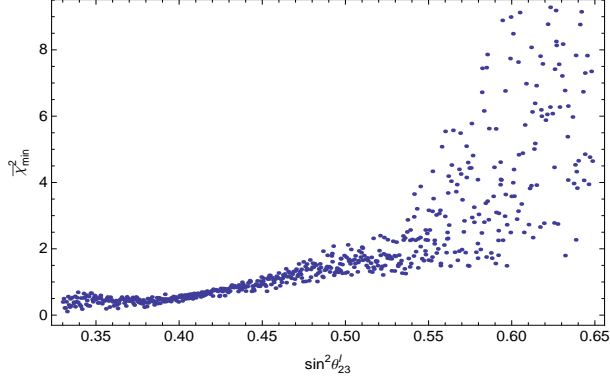


FIG. 1. Variation of $\bar{\chi}_{min}^2$ with $\sin^2 \theta_{23}^l$ in the minimal non-susy $SO(10)$ model with Type-I seesaw.

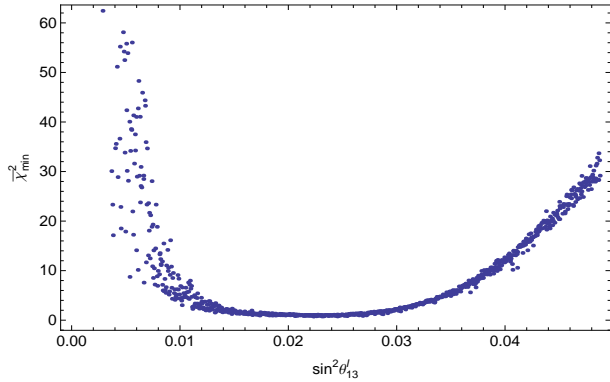


FIG. 2. Variation of $\bar{\chi}_{min}^2$ with $\sin^2 \theta_{13}^l$ in the minimal non-susy $SO(10)$ model with Type-I seesaw.

several new parameters.

The fermion mass relations in this model are given by eq.(5) with $H = 0$. F can be made real diagonal without loss of generality. M_l is not diagonal and the charged lepton masses are included in the χ^2 function (8) unlike the previous case of the minimal model where they were set as input. Since the errors in the charged lepton masses are extremely small, the numerical optimization algorithm we use is unable to converge to the solution in finite time. Thus we set 10% error in charged lepton masses and minimize the χ^2 with respect to 16 (3 in F , 6 in G , real s and complex t_l, t_u, t_D) real parameters.

Results of numerical analysis carried out separately for type-I and type-II dominated seesaw scenarios are shown in Table(VIII). The detailed fits are quite different in two cases showing that a simple proportionality of the type-II and type-I contribution observed in the two generation study [26] does not hold in general. The model fails badly in reproducing the fermion mass spectrum in either case. Analytic study of the two generations lead in the model to a relation $m_\tau \approx 3m_b$. This is born out in the detailed numerical study with three generations as well. But this relation becomes one of the causes of the failure of the model as is clearly seen in the Table (VIII). Likewise, the numerical fits lead to nearly

Observables	Type-I		Type-II	
	Fitted value	pull	Fitted value	pull
m_d	0.000186192	-1.9871	0.000223284	-1.90982
m_s	0.00267758	-3.2204	0.00296063	-3.17323
m_b	0.844022	-3.89946	0.836471	-4.08822
m_u	0.00048096	0.00480131	0.000483412	0.0170595
m_c	0.23454	-0.0135291	0.237869	0.0819818
m_t	74.053	0.0132566	73.891	-0.0294532
m_e	0.000467656	-0.0424983	0.000475465	0.123771
m_μ	0.0964545	-0.271534	0.101839	0.271587
m_τ	2.61149	5.49314	2.60147	5.43367
$\left(\frac{\Delta m_{sol}^2}{\Delta m_{atm}^2}\right)$	0.0303749	0.0605819	8.59×10^{-7}	-13.4841
$\sin \theta_{12}^q$	0.224581	-0.0172464	0.224591	-0.00790894
$\sin \theta_{23}^q$	0.0419722	-0.0218756	0.0420623	0.0490417
$\sin \theta_{13}^q$	0.00354561	0.0948516	0.00353062	0.0393252
$\sin^2 \theta_{12}^l$	0.321216	0.0243762	0.320612	-0.0124452
$\sin^2 \theta_{23}^l$	0.450311	-0.0544896	0.0375094	-8.59228
δ_{CKM}	69.5526	-0.0234639	69.5794	-0.0153481
χ^2		59.7934		315.705

TABLE VIII. Best fit solutions for fermion masses and mixing obtained assuming the type-I and type-II seesaw dominance in non-SUSY $SO(10)$ model with $120 + \overline{126}$ Higgs. All the masses shown are in GeV units. Various observables and their pulls at the minimum are shown.

vanishing solar scale at the minimum in the type-II case. This becomes an added cause of very poor fits. It appears from the results that the renormalizable model with $45 + 120 + \overline{126}$ Higgs fields is not a good candidate to obtain even fermion mass spectrum in spite of its attractiveness at the two generation level [26].

C. Numerical Analysis: Model with $10 + \overline{126} + 120$ Higgs fields.

As before, we consider the case with Hermitian (Dirac) mass matrices. The mass relations are same as in eq.(5) with all parameters real. We have chosen the basis with a diagonal H . M_l is not diagonal in this basis and we parameterize it as $M_l = U_l D_l U_l^\dagger$ with U_l being a general unitary matrix expressed in terms of three angles and six phases and D_l is a diagonal matrix for the charged lepton masses. One can rewrite M_l in eq.(5) as

$$3F - it_l G = H - U_l D_l U_l^\dagger$$

Since F and G are real, the real and imaginary parts of the RHS separately determine F and $t_l G$ in terms of the charged lepton masses and parameters of H and U_l which are put back in eq.(5). The remaining fermion mass matrices can be expressed in terms of 17 (3 in H , 9 in U_l , real r, s, t_l, t_u, t_D) real parameters in the case of type-I seesaw dominance which determine 16 observables P_i shown in Table(VI). One parameter t_D becomes irrelevant for the type-II seesaw case. We do the numerical analysis for this case and results are shown in Table(IX).

Observables	Type-I		Type-II	
	Fitted value	pull	Fitted value	pull
m_d	0.00113968	-0.000676838	0.00108711	-0.110189
m_s	0.0219909	-0.00150966	0.0142689	-1.28852
m_b	1.	0.0000376219	1.19665	4.9162
m_u	0.000480133	0.000666686	0.000486627	0.0331338
m_c	0.235007	0.000211758	0.240819	0.166268
m_t	73.9997	-0.0000888053	77.4295	0.857367
m_e	0.000469652	0	0.000469652	0
m_μ	0.0991466	0	0.0991466	0.220249
m_τ	1.68558	0	1.68558	0.000124065
$\left(\frac{\Delta m_{sol}^2}{\Delta m_{atm}^2}\right)$	0.0302402	0.000545016	0.0260106	-1.88556
$\sin \theta_{12}^q$	0.224601	0.00105776	0.224567	-0.0304356
$\sin \theta_{23}^q$	0.0420001	0.0000431604	0.0431393	0.897068
$\sin \theta_{13}^q$	0.00351992	-0.000308192	0.00338234	-0.509862
$\sin^2 \theta_{12}^l$	0.320821	0.000292661	0.278093	-2.6052
$\sin^2 \theta_{23}^l$	0.453034	0.000947066	0.343286	-2.26804
$\sin^2 \theta_{13}^l$	0.0306736	-	0.00538748	-
$\delta_{CKM}[\circ]$	69.6278	-0.000660788	72.7155	0.935014
$\delta_{MNS}[\circ]$	355.719	-	46.8148	-
$\alpha_1[\circ]$	60.079	-	60.6202	-
$\alpha_2[\circ]$	214.691	-	250.978	-
$r_{R(L)}$	1.56×10^{-15}	-	3.43×10^{-10}	-
χ^2		$\sim 10^{-6}$		44.0801

TABLE IX. Best fit solutions for fermion masses and mixing obtained assuming the type-I and type-II seesaw dominance in the non-supersymmetric $SO(10)$ model with $10 + \overline{126} + 120$ Higgs. Various observables and their pulls at the minimum are shown. All the masses shown are in GeV units. The bold faced quantities are predictions of the respective solutions.

Parameters obtained for the best fit solutions in type-I case are shown in Appendix B. Unlike the supersymmetric case, the presence of 120_H does not help in improving the fits

in the type-II seesaw dominated case. But the fits obtained for the type-I scenario are considerably better compared to the corresponding supersymmetric as well as the minimal non-supersymmetric case. Pulls in all observables are practically zero in this case.

The predictions of the model for the observables $\sin^2 \theta_{23}^l$ and $\sin^2 \theta_{13}^l$ are displayed in Fig.3 and Fig.4 respectively. Once again a clear prediction $\sin^2 \theta_{13} \gtrsim 0.015$ emerges in this case.

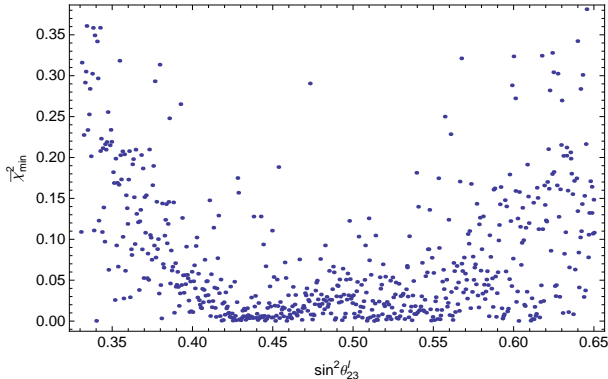


FIG. 3. Variation of $\bar{\chi}_{min}^2$ with $\sin^2 \theta_{23}^l$ in the extended model with Type-I seesaw.

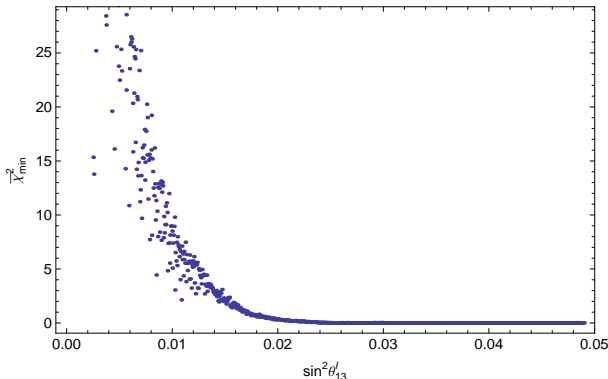


FIG. 4. Variation of $\bar{\chi}_{min}^2$ with $\sin^2 \theta_{13}^l$ in the extended model with Type-I seesaw.

V. NUMERICAL ANALYSIS AND UNDERLYING FLAVOUR STRUCTURE

Numerical analysis presented in the previous section has demonstrated viability of various $SO(10)$ models in explaining the fermion masses and mixing. In the process, it has also provided us with specific structure of fermion mass matrices which can be used to obtain some insight into the underlying flavour structure. We discuss one specific case namely, the minimal non-supersymmetric model from this point of view.

At the $SO(10)$ level, Yukawa couplings H, F, G determine the flavour structure of various mass matrices. Thus any underlying flavour symmetry if it exists should get reflected in

the structure of these matrices. Specific structures for the Yukawa coupling matrices have been used to predict relations between the (hierarchical) quark masses and (small) quark mixing, see for example [23, 30, 31]. In a large class of such models, the observed masses and mixing patterns among quarks are reproduced when elements of the quark mass matrices are expressed as powers of one or two expansion parameters. Following this, we try to look for a similar parameterization for the underlying matrices F, H in case of the minimal non-supersymmetric model. We choose the Cabibbo angle $\lambda = 0.2246$ as a convenient parameter. Elements of F and H in this case are then found to have the following hierarchical structure in the basis with a diagonal M_I :

$$\begin{aligned}
H &= 1.088e^{0.435i} \text{ GeV} \begin{pmatrix} 0.513e^{1.659i}\lambda^4 & 0.361e^{-1.257i}\lambda^3 & 0.685e^{0.843i}\lambda^2 \\ 0.361e^{-1.257i}\lambda^3 & 0.119e^{1.143i}\lambda^2 & 0.490e^{-2.123i}\lambda \\ 0.685e^{0.843i}\lambda^2 & 0.490e^{-2.123i}\lambda & 1 \end{pmatrix}, \\
F &= 0.278e^{2.561i} \text{ GeV} \begin{pmatrix} 0.802e^{-0.226i}\lambda^4 & 0.470e^{2.90i}\lambda^3 & 0.892e^{-1.283i}\lambda^2 \\ 0.470e^{2.90i}\lambda^3 & 2.359e^{0.515i}\lambda^2 & 0.639e^{2.034i}\lambda \\ 0.892e^{-1.283i}\lambda^2 & 0.639e^{2.034i}\lambda & 1 \end{pmatrix} \quad (14)
\end{aligned}$$

33 element turns out to be largest both for F and H and we have normalized other elements by its value in writing the above structure. Most coefficients in powers of λ are roughly $\mathcal{O}(1)$ except for the 22 elements.

The above structure determined numerically here is suggestive of an underlying $U(1)$ symmetry used [32] in the Froggatt Nielsen (FG) approach. Indeed a simple $U(1)$ can explain the occurrence of various powers of λ in eq.(14). Consider a $U(1)$ symmetry with the $U(1)$ charges 2, 1, 0 assigned respectively to three generations of 16_F -plet. Both 10_H and $\overline{126}_H$ are assumed neutral under this symmetry. In this case, the 33 elements of F, H arise from the renormalizable couplings $16_{3F}16_{3F}\phi_H$ ($\phi = 10, \overline{126}$). The 23 and 32 elements follow from the couplings $16_{2F}16_{3F}\phi_H\frac{\eta}{M}$. Likewise, the two, three and four powers of η respectively generate $\mathcal{O}(\lambda^2, \lambda^3, \lambda^4)$ terms in eq.(14) where $\lambda = \frac{\langle\eta\rangle}{M}$, M being some underlying scale above the $U(1)$ breaking scale $\langle\eta\rangle$ and η is assumed to carry the $U(1)$ charge -1 . The quark mass matrices resulting from the above F, H also follow this simple pattern as in eq.(14):

$$\begin{aligned}
M_d &= 0.9708e^{0.6809i} \text{ GeV} \begin{pmatrix} 0.800e^{1.481i}\lambda^4 & 0.539e^{-1.503i}\lambda^3 & 1.024e^{0.597i}\lambda^2 \\ 0.539e^{-1.503i}\lambda^3 & 0.699e^{2.204i}\lambda^2 & 0.733e^{-2.370i}\lambda \\ 1.024e^{0.597i}\lambda^2 & 0.733e^{-2.370i}\lambda & 1 \end{pmatrix}, \\
M_u &= 72.639e^{0.523i} \text{ GeV} \begin{pmatrix} 0.609e^{1.585i}\lambda^4 & 0.419e^{-1.359i}\lambda^3 & 0.796e^{0.741i}\lambda^2 \\ 0.419e^{-1.359i}\lambda^3 & 0.281e^{1.981i}\lambda^2 & 0.570e^{-2.225i}\lambda \\ 0.796e^{0.741i}\lambda^2 & 0.570e^{-2.225i}\lambda & 1 \end{pmatrix}
\end{aligned}$$

This structure is already proposed and studied in [31] as a possible explanation of quark and neutrino mixing and masses. Here it follows from a detailed analysis of this specific $SO(10)$ model. As shown in [31], such a form can reproduce the observed mixing and mass patterns for quarks. The expansion parameter chosen in [31] is somewhat larger, $\lambda = 0.26$. The Dirac neutrino mass matrix on the other hand is given by

$$M_D = 86.240e^{0.210i} \text{ GeV} \begin{pmatrix} 0.253e^{1.795i}\lambda^4 & 0.201e^{-0.959i}\lambda^3 & 0.382e^{1.140i}\lambda^2 \\ 0.201e^{-0.959i}\lambda^3 & 0.567e^{-0.222i}\lambda^2 & 0.273e^{-1.825i}\lambda \\ 0.382e^{1.140i}\lambda^2 & 0.273e^{-1.825i}\lambda & 1 \end{pmatrix} \quad (15)$$

The coefficients in front of various elements are anomalously small and thus M_D does not really share the same symmetry as the underlying Yukawa matrices. The M_D and $M_R \sim F$ conspire to produce a neutrino mass matrix which has an interesting form

$$M_\nu = 0.087e^{-0.898i} r_R r^2 \text{ GeV} \begin{pmatrix} 1.339e^{2.543i}\lambda^3 & 0.878126e^{-0.662i}\lambda^2 & 1.753e^{1.529i}\lambda \\ 0.878e^{-0.662i}\lambda^2 & 0.800e^{-2.646i} & 1.062e^{-1.458i} \\ 1.753e^{1.529i}\lambda & 1.062e^{-1.458i} & 1 \end{pmatrix} \quad (16)$$

Since we are working in a basis with a diagonal M_l , the above matrix determines physical neutrino mixing and allows us to understand the leptonic mixing structure analytically. Firstly, the 23 block has all elements of $\mathcal{O}(1)$ which results in the large atmospheric angle and hierarchy in neutrino masses. Secondly, the 11 and 12 elements are zero to leading order in λ . In the approximation of neglecting higher powers of λ , the M_ν has two-zero texture (classified as A1 in [33]). The presence of the zeros leads to a firm prediction of the third mixing angle [33]

$$\sin^2 \theta'_{13} \approx \left(\frac{\Delta m_{sol}^2}{\Delta m_{atm}^2} \right) \frac{\sin^2 \theta'_{12} \cos^2 \theta'_{12}}{\cos 2\theta'_{12} \tan^2 \theta'_{23}}. \quad (17)$$

This analytic relation is in very good agreement with the numerical values. Evaluation of the RHS using the best fit values of parameters in Table(VII) leads to $\sin^2 \theta'_{13} \approx 0.0245$ in agreement with the numerical prediction. Even away from the minimum χ^2 , one would get $\sin^2 \theta'_{13}$ around 0.02 as long as two zero structure and hence eq.(17) holds approximately. This is born out quite well in Figure 2.

The simple $U(1)$ symmetry used to explain the structure of F, H may appear to have two shortcomings. Firstly, the specific structures are found in a basis with a diagonal M_l . Secondly, the coefficients of powers of λ in F, H are not strictly $\mathcal{O}(1)$, notably in the 22 elements. In general, the definition of symmetry and resulting texture of Yukawa matrices are basis dependent. Basis with a diagonal M_l are very special basis and it would be more desirable to find a basis in which M_l also has a structure similar to the F, H, M_d, M_u . One can indeed find a class of unitary rotations which bring the diagonal M_l to the form as in eq.(14) and at the same time retain the forms of F, H albeit with a different set of coefficients.

The $U(1)$ symmetry leads to the following general form of the Yukawa matrices:

$$(F, H) = a_{33}^{F,H} \begin{pmatrix} a_{11}^{F,H} \lambda^4 & a_{12}^{F,H} \lambda^3 & a_{13}^{F,H} \lambda^2 \\ a_{12}^{F,H} \lambda^3 & a_{22}^{F,H} \lambda^2 & a_{23}^{F,H} \lambda \\ a_{13}^{F,H} \lambda^2 & a_{23}^{F,H} \lambda & 1 \end{pmatrix}. \quad (18)$$

F, H as given above can be diagonalized with high accuracy by rotation $R_{F,H}$ consisting of three successive rotations in 2 – 3, 1 – 3 and 1 – 2 plane with the mixing angles [31]

$$\begin{aligned} \sin \theta_{23}^{F,H} &\approx a_{23}^{F,H} \lambda, \\ \sin \theta_{13}^{F,H} &\approx a_{13}^{F,H} \lambda^2, \\ \tan 2\theta_{12}^{F,H} &\approx 2\lambda \frac{a_{12}^{F,H} - a_{23}^{F,H} a_{13}^{F,H}}{a_{22}^{F,H} - (a_{23}^{F,H})^2 + \mathcal{O}(\lambda^2)} \end{aligned} \quad (19)$$

The eigenvalues of F, H are $\mathcal{O}(1, \lambda^2, \lambda^4)$. The eigenvalues of M_l are roughly of similar order-though the coefficient for the electron mass is somewhat small. Thus M_l can be put to the form as in (14) by rotating the diagonal M_l with a rotation matrix V_l with angles as in eq.(19) but with a different set of coefficients a_{ij}^l . It is easy to see that when F, H are expressed in new basis their forms do not change to leading order in λ but now coefficients in front of powers of λ are different say, $a_{ij}^{lF,H}$. They depend on $a_{ij}^{F,H}$ and a_{ij}^l . Thus symmetry in question may manifest itself in more general basis than the specific diagonal basis provided $a_{ij}^{lF,H}$ are also $\mathcal{O}(1)$.

Let us consider a simple example. Rotate F, H and diagonal M_l with a common rotation V_l defined as

$$V_l = \begin{pmatrix} 1 & 0 & 0 \\ 0 & 1 - 1/2\lambda^2 & \lambda e^{i\beta} \\ 0 & -\lambda e^{-i\beta} & 1 - 1/2\lambda^2 \end{pmatrix}$$

β can be chosen such that the coefficient of various powers of λ in elements of $F' = V_l^T F V_l$ and $H' = V_l H V_l$ are near to 1. The best fit value of β turns out to be $\beta = 1.055$ and for this one gets

$$\begin{aligned} |F'| &= 0.278 \text{ GeV} \begin{pmatrix} 0.802\lambda^4 & 0.772\lambda^3 & 0.892\lambda^2 \\ 0.772\lambda^3 & 1.12\lambda^2 & 1.638\lambda \\ 0.892\lambda^2 & 1.638\lambda & 1 \end{pmatrix} \\ |H'| &= 1.088 \text{ GeV} \begin{pmatrix} 0.513\lambda^4 & 0.593\lambda^3 & 0.685\lambda^2 \\ 0.593\lambda^3 & 0.939\lambda^2 & 0.876\lambda \\ 0.685\lambda^2 & 0.876\lambda & 1 \end{pmatrix} \end{aligned} \quad (20)$$

Unlike in eq.(14), all the coefficients of various elements in the above equation are now $\mathcal{O}(1)$.

M_l is non-diagonal in this basis and is given by

$$|M_l| = 1.685\text{GeV} \begin{pmatrix} 0.109\lambda^4 & 0 & 0 \\ 0 & 1.06\lambda^2 & 1.006\lambda \\ 0 & 1.006\lambda & 1 \end{pmatrix}. \quad (21)$$

We note that the Yukawa coupling matrices in cases other than the minimal also display hierarchical structure, see results in Appendix (B). Thus these cases can also be understood in terms of some simple pattern as in the minimal case discussed here explicitly.

VI. SUMMARY

$SO(10)$ models have been used to obtain a unified description of fermion masses and mixing angles. We have undertaken in this paper an exhaustive analysis of many different $SO(10)$ models. Using several different data sets as input, we have numerically determined viability of these models in reproducing the fermion spectrum. In case of the supersymmetric models, we used data corresponding to different values of $\tan\beta$ and with or without appreciable finite threshold correction. Comparison of different set clearly brings out an important feature. In the minimal model with type-II seesaw dominance, the b - τ unification appears to be a key ingredient. The cases without such unification cannot explain the entire fermion spectrum. In particular, the case of very low $\tan\beta$ showing this unification works much better than the previously studied data set with $\tan\beta = 10$. This connection is not required if neutrinos obtain their masses from the type-I seesaw mechanism. In this case one can obtain very good fits in the minimal model almost for every data set used, see Tabel(III). Moreover, the $B - L$ breaking scale inferred from neutrino masses also lies closer to the GUT scale compared to the type-II seesaw mechanism. The situation becomes better when a 120-plet of Higgs field is added to the model. Here one can get excellent fits to fermion masses in both the type-I and type-II seesaw mechanisms.

We also carried out a detailed analysis of the fermion masses in non-supersymmetric models. The minimal non-supersymmetric model with $45_H + 10_H + \overline{126}_H$ is quite economical and is argued recently [16, 17] to be a viable candidate for the gauge coupling unification. As shown here it also provides a very good description of fermion masses as well. Intermediate scale $\sim 10^{11}$ GeV is required in this model in order to obtain the unification of gauge coupling [16]. The scale preferred from the fits to fermion masses presented here is somewhat larger. This scale can be reduced if the admixture of the light doublet in the doublet component of $\overline{126}_H$ is very small, see eq.(12). Viability of these as well as simultaneous analysis of the constraint from the gauge coupling unification will depend on the detailed analysis of the scalar sector of the theory. The Yukawa coupling matrices obtained numerically in this case display interesting structure which can be understood from a very simple symmetry imposed at a high scale. These features coupled with its economy makes the minimal non

supersymmetric model an attractive choice to unify basic gauge and Yukawa interactions.

Acknowledgements

Computations needed for the results reported in this work were done using the PRL 3TFLOP cluster at Physical Research Laboratory, Ahmedabad. K.M.P. would like to thank Dr. Dilip K. Angom for providing useful tips on parallel computing.

VII. APPENDIX

We list here the fermion mass matrices using the best fit values of the parameters given in Table VII (Table IX) corresponding to the type-I seesaw mechanism in the case of minimal (non-minimal) non-supersymmetric $SO(10)$ model. All the mass matrices are expressed in GeV units.

A. Best fit parameter values: The minimal nonsusy $SO(10)$ model, type-I seesaw mechanism (Table VII).

Parameters obtained for best fit solution.

$$\begin{aligned}
 r &= 69.1739; \quad s = 0.362941 - 0.0463175i \\
 M_l &= \begin{pmatrix} 0.000469652 & 0 & 0 \\ 0 & 0.0991466 & 0 \\ 0 & 0 & 1.68558 \end{pmatrix} \\
 M_d &= \begin{pmatrix} -0.00110182 + 0.00164125i & 0.0040374 - 0.00434507i & 0.0145011 + 0.0480084i \\ 0.0040374 - 0.00434507i & -0.0331074 + 0.00870484i & -0.0187112 - 0.158707i \\ 0.0145011 + 0.0480084i & -0.0187112 - 0.158707i & 0.754282 + 0.611126i \end{pmatrix} \quad (22)
 \end{aligned}$$

Results:

$$\begin{aligned}
 M_u &= \begin{pmatrix} -0.0575896 + 0.0967087i & 0.231322 - 0.25593i & 0.881792 + 2.78041i \\ 0.231322 - 0.25593i & -0.826159 + 0.612181i & -1.21531 - 9.21493i \\ 0.881792 + 2.78041i & -1.21531 - 9.21493i & 62.9262 + 36.2872i \end{pmatrix} \\
 M_\nu &= r_R r^2 \begin{pmatrix} -0.0000981928 + 0.00131563i & 0.0000421662 - 0.003853i & 0.0276444 + 0.0202258i \\ 0.0000421662 - 0.003853i & -0.0640659 + 0.0272358i & -0.0653091 - 0.0653272i \\ 0.0276444 + 0.0202258i & -0.0653091 - 0.0653272i & 0.054234 - 0.0680089i \end{pmatrix}
 \end{aligned}$$

B. Best fit parameter values: The non-minimal nonsusy $SO(10)$ model, type-I seesaw mechanism (Table IX).

Parameters obtained for best fit solution.

$$\begin{aligned}
 r &= -52.4173; \quad s = 1.61949; \quad t_l = 3.1751; \quad t_u = 0.0413014; \quad t_D = -11.7339. \\
 H &= \begin{pmatrix} 0.00158452 & 0 & 0 \\ 0 & 0.0407501 & 0 \\ 0 & 0 & -0.330398 \end{pmatrix} \\
 F &= \begin{pmatrix} -0.00116221 & -0.000145513 & 0.0130876 \\ -0.000145513 & -0.0224155 & -0.00121344 \\ 0.0130876 & -0.00121344 & -0.667509 \end{pmatrix} \\
 G &= \begin{pmatrix} 0 & -0.00670763 & 0.00612927 \\ 0.00670763 & 0 & -0.0437162 \\ -0.00612927 & 0.0437162 & 0 \end{pmatrix} \tag{23}
 \end{aligned}$$

Results:

$$\begin{aligned}
 M_d &= \begin{pmatrix} 0.00042231 & -0.000145513 - 0.00670763i & 0.0130876 + 0.00612927i \\ -0.000145513 + 0.00670763i & 0.0183346 & -0.00121344 - 0.0437162i \\ 0.0130876 - 0.00612927i & -0.00121344 + 0.0437162i & -0.997907 \end{pmatrix} \\
 M_u &= \begin{pmatrix} 0.0156028 & 0.0123525 + 0.0145214i & -1.11099 - 0.0132693i \\ 0.0123525 - 0.0145214i & -0.233181 & 0.103008 + 0.0946413i \\ -1.11099 + 0.0132693i & 0.103008 - 0.0946413i & 73.9827 \end{pmatrix} \\
 M_l &= \begin{pmatrix} 0.00507117 & 0.00043654 - 0.0212974i & -0.0392628 + 0.019461i \\ 0.00043654 + 0.0212974i & 0.107997 & 0.00364033 - 0.138803i \\ -0.0392628 - 0.019461i & 0.00364033 + 0.138803i & 1.67213 \end{pmatrix} \\
 M_\nu &= r_R r^2 \begin{pmatrix} 0.243898 + 0.00702837i & 0.0907917 - 0.0237474i & -1.65214 - 0.184893i \\ 0.0907917 - 0.0237474i & 4.6052 - 0.0433382i & -5.76376 + 0.720305i \\ -1.65214 - 0.184893i & -5.76376 + 0.720305i & 5.33677 + 1.11414i \end{pmatrix} \tag{24}
 \end{aligned}$$

-
- [1] C.S. Aulakh, R.N. Mohapatra, Phys. Rev. D **28**, 217 (1983);
T. E. Clark, T. K. Kuo and N. Nakagawa, Phys. Lett. B **115**, 26 (1982);
K.S. Babu, R.N. Mohapatra, Phys. Rev. Lett. **70**, 2845 (1993) [arXiv:hep-ph/9209215];
K. Matsuda, Y. Koide, T. Fukuyama, Phys. Rev. D **64**, 053015 (2001) [arXiv:hep-ph/0010026];
K. Matsuda, Y. Koide, T. Fukuyama and H. Nishiura, Phys. Rev. D **65**, 033008 (2002)
[Erratum-ibid. D **65**, 079904 (2002)] [arXiv:hep-ph/0108202];
T. Fukuyama and N. Okada, JHEP **0211**, 011 (2002) [arXiv:hep-ph/0205066].

- [2] H. S. Goh, R. N. Mohapatra and S. Nasri, Phys. Rev. D **70**, 075022 (2004) [arXiv:hep-ph/0408139];
A. Melfo, A. Ramirez and G. Senjanovic, Phys. Rev. D **82**, 075014 (2010) [arXiv:1005.0834 [hep-ph]].
- [3] B. Bajc, G. Senjanovic and F. Vissani, Phys. Rev. Lett. **90**, 051802 (2003) [arXiv:hep-ph/0210207].
- [4] H.S. Goh, R.N. Mohapatra, S.P. Ng, Phys. Lett. B **570**, 215 (2003) [arXiv:hep-ph/0303055];
H.S. Goh, R.N. Mohapatra, S.P. Ng, Phys. Rev. D **68**, 115008 (2003) [arXiv:hep-ph/0308197];
C. S. Aulakh and S. K. Garg, Nucl. Phys. B **757**, 47 (2006) [arXiv:hep-ph/0512224];
B. Bajc, A. Melfo, G. Senjanovic and F. Vissani, Phys. Lett. B **634**, 272 (2006) [arXiv:hep-ph/0511352];
B. Bajc, I. Dorsner and M. Nemevsek, JHEP **0811**, 007 (2008) [arXiv:0809.1069 [hep-ph]].
- [5] S. Bertolini, M. Malinský, Phys. Rev. D **72**, 055021 (2005) [arXiv:hep-ph/0504241];
C. S. Aulakh, B. Bajc, A. Melfo, G. Senjanovic and F. Vissani, Phys. Lett. B **588**, 196 (2004) [arXiv:hep-ph/0306242];
K.S. Babu, C. Macesanu, Phys. Rev. D **72**, 115003 (2005) [arXiv:hep-ph/0505200];
B. Bajc, A. Melfo, G. Senjanovic and F. Vissani, Phys. Rev. D **70**, 035007 (2004) [arXiv:hep-ph/0402122].
- [6] S. Bertolini, T. Schwetz and M. Malinsky, Phys. Rev. D **73**, 115012 (2006) [arXiv:hep-ph/0605006].
- [7] C. S. Aulakh and A. Girdhar, Int. J. Mod. Phys. A **20**, 865 (2005) [arXiv:hep-ph/0204097];
C. S. Aulakh and A. Girdhar, Nucl. Phys. B **711**, 275 (2005) [arXiv:hep-ph/0405074];
T. Fukuyama, A. Ilakovac, T. Kikuchi, S. Meljanac and N. Okada, J. Math. Phys. **46**, 033505 (2005) [arXiv:hep-ph/0405300];
T. Fukuyama, A. Ilakovac, T. Kikuchi, S. Meljanac and N. Okada, Phys. Rev. D **72**, 051701 (2005) [arXiv:hep-ph/0412348];
C. S. Aulakh, Phys. Rev. D **72**, 051702 (2005) [arXiv:hep-ph/0501025];
C. S. Aulakh and S. K. Garg, arXiv:0710.4018 [hep-ph].
- [8] C. S. Aulakh and S. K. Garg, arXiv:0807.0917 [hep-ph];
C. S. Aulakh, Phys. Lett. B **661**, 196 (2008) [arXiv:0710.3945 [hep-ph]];
N. Oshimo, Phys. Rev. D **66**, 095010 (2002) [arXiv:hep-ph/0206239];
N. Oshimo, Nucl. Phys. B **668**, 258 (2003) [arXiv:hep-ph/0305166];
B. Dutta, Y. Mimura and R. N. Mohapatra, Phys. Rev. Lett. **94**, 091804 (2005) [arXiv:hep-ph/0412105];
B. Dutta, Y. Mimura and R. N. Mohapatra, Phys. Rev. D **72**, 075009 (2005) [arXiv:hep-ph/0507319];
W. M. Yang and Z. G. Wang, Nucl. Phys. B **707**, 87 (2005) [arXiv:hep-ph/0406221].
- [9] A. S. Joshipura, B. P. Kodrani and K. M. Patel, Phys. Rev. D **79**, 115017 (2009) [arXiv:0903.2161 [hep-ph]].

- [10] W. Grimus and H. Kuhbock, Phys. Lett. B **643**, 182 (2006) [arXiv:hep-ph/0607197].
- [11] W. Grimus and H. Kuhbock, Eur. Phys. J. C **51**, 721 (2007) [arXiv:hep-ph/0612132].
- [12] S. Bertolini, M. Frigerio, M. Malinský, Phys. Rev. D **70**, 095002 (2004) [arXiv:hep-ph/0406117];
S. Bertolini and M. Malinsky, Phys. Rev. D **72**, 055021 (2005) [arXiv:hep-ph/0504241].
- [13] B. Dutta, Y. Mimura and R. N. Mohapatra, Phys. Lett. B **603**, 35 (2004) [arXiv:hep-ph/0406262].
- [14] C. S. Aulakh, arXiv:hep-ph/0602132;
C. S. Aulakh and S. K. Garg, arXiv:hep-ph/0612021.
- [15] G. Altarelli and G. Blankennurg, arXiv:1012.2697v1.
- [16] S. Bertolini, L. Di Luzio and M. Malinsky, Phys. Rev. D **80**, 015013 (2009) [arXiv:0903.4049 [hep-ph]].
- [17] S. Bertolini, L. Di Luzio, M. Malinsky, Phys. Rev. D **81**, 035015 (2010) [arXiv:0912.1796 [hep-ph]].
- [18] N. G. Deshpande, E. Keith and P. B. Pal, Phys. Rev. D **47** 2892 (1993).
- [19] G. Anasatze, J. P. Derendinger and F. Buccella, Z. Phys. C **20** 269 (1983);
K. S. Babu and E. Ma, Phys. Rev. D **31** 2316 (1985);
M. Yasue, Phys. Lett. B **103** 33(1981); Phys. Rev. D **24** 1005 (1981).
- [20] H. Georgi and C. Jarlskog, Phys. Lett. B **86** 297 (1979).
- [21] C. R. Das and M. K. Parida, Eur. Phys. J. C **20** 121(2001)[ArXiv:hep-ph/0010004].
- [22] Z. z. Xing, H. Zhang and S. Zhou, Phys. Rev. D **77**, 113016 (2008) [arXiv:0712.1419 [hep-ph]].
- [23] G. Ross and M. Serna, Phys. Lett. B **664**, 97 (2008) [arXiv:0704.1248 [hep-ph]].
- [24] S. Antusch and M. Spinrath, Phys. Rev. D **78**, 075020 (2008) [arXiv:0804.0717 [hep-ph]].
- [25] R. Dermisek and S. Raby, Phys. Lett. B **622** 327 (2005)[arXiv:hep-ph/0507045];
R. Dermisek M. Harada and S. Raby, Phys. Rev. D **74** 035011 (2006)[arXiv:hep-ph/0606055];
C. H. Albright and S. M. Barr, Phys. Rev. D **62** 093008[arXiv:hep-ph/0104294];
C. H. Albright, K. S. Babu and S. M. Barr, Nucl. Phys. Proc. Suppl. **77**, 308 (1999) [arXiv:hep-ph/9805266].
- [26] B. Bajc, A. Melfo, G. Senjanovic and F. Vissani, Phys. Rev. D **73**, 055001 (2006) [arXiv:hep-ph/0510139].
- [27] Our notations for the quark and leptonic mixing angles and phases are as in, C. Amsler et al. (Particle Data Group), Physics Letters B **667**, 1 (2008). Quark and lepton mixing angles are distinguished by superscript q and l respectively.
- [28] M. C. Gonzalez-Garcia, M. Maltoni and J. Salvado, JHEP **1004**, 056 (2010) [arXiv:1001.4524 [hep-ph]].
- [29] T. Blazek, S. Raby and S. Pokorski, Phys. Rev. D **52** 4151 (1995).
- [30] R. G. Roberts, A. Romanino, G. G. Ross and L. Velasco-sevilla, Nucl. Phys. B **615** 358 (2001)[ArXiv:hep-ph/0104088].
- [31] I. Dorsner and A. Y. Smirnov, Nucl. Phys. B **698**, 386 (2004) [arXiv:hep-ph/0403305].

- [32] C. D. Froggatt and H. B. Nielsen, Nucl. Phys. B **147**, 277 (1979).
- [33] P. H. Frampton, S. L. Glashow and D. Marfatia, Phys. Lett. B **536**, 79 (2002)
[arXiv:hep-ph/0201008].

